# Prediction of Wave-Induced Surge Force Using Overset Grid RANS Solver

Hirotada Hashimoto, *Kobe University*, hashimoto@port.kobe-u.ac.jp

Shota Yoneda, *Kobe University*, s_yoneda@maritime.kobe-u.ac.jp

Yusuke Tahara, *National Maritime Research Institute*, tahara@nmri.go.jp

Eiichi Kobayashi, *Kobe University*, kobayasi@maritime.kobe-u.ac.jp

**ABSTRACT**

Prediction of the wave surging force acting on a ship in following seas is a key issue for the accurate prediction of surf-riding phenomenon. It is pointed out that the linear Froude-Krylov component generally overestimates the amplitude of wave-induced surge force. Therefore a simple correction formula for the Froud-Krylov force is proposed in the second-generation intact stability criteria under discussed at IMO. In this study, a RaNS solver with an overset grid system is used to realize more accurate prediction of the wave-induced surge force. Then the current correction formula is evaluated based on the CFD results for a series of hull forms with variety of hull form parameters.

**Keywords:** *Second-generation intact stability criteria, Broaching/Surf-riding, Wave-induced surge force, Overset grid RaNS Solver, Froude-Krylov force, Correction formula*

## 1. INTRODUCTION

The second-generation intact stability criteria are under development at International Maritime Organization (IMO). There are five stability failure modes to be discussed, and experimental/numerical prediction of the wave-induced surge force in following and quartering waves became an important issue for relatively high-speed vessels because it has big influence on the threshold of surf-riding and near surf-riding condition, which are triggers for dangerous situations of broaching and pure loss of stability. In a conventional way, the wave-induced surge force is calculated as the Froude-Krylov force. However its accuracy is not satisfactory for a criteria-use purpose because it generally provides the larger amplitude of the wave-induced surge force, and hence the danger of broaching and pure loss of stability could be overestimated. Therefore more reliable approach is needed for the second-generation intact stability criteria for surf-riding/broaching, i.e. alternative to captive model experiments to measure the wave-induced surge force. In the prediction of the wave-induced surge force for a ship running in following seas, considering the effects of diffraction and ship motion could be candidates to improve the prediction accuracy, and a three-dimensional hydrodynamic effect is also a possible element, which are missing in the linear Froude-Krylov calculation based on the strip theory.

Following these situations, CFD (Computational Fluid Dynamics) simulation to estimate the wave-induced surge force in following waves is executed using an overset grid RaNS Solver (CFDShip Iowa ver.4.5). In this study, the ONR tumblehome vessel is used as a sample ship and the CFD results are

compared with an existing experimental result. As a result, it is well confirmed that the CFD provides more accurate prediction than the Froude-Krylov component and the CFD results show fairy good agreement with the experimental results in a sense of practical uses. Then further CFD-based studies are done for a series of ONR-tumblehome hulls with varieties of fineness coefficients to investigate the influence of the hull form on the wave-induced surge force, and then the current correction formula for the Froude-Krylov component in the level 2 vulnerability criterion for broaching, is evaluated.

## 2. SECOND-GENERATION INTACT STABILITY CRITERIA

In the level 2 vulnerability criterion for broaching, the amplitude of the wave-induced surging force is calculated as the linear Froude-Krylov force by Eq.1 (IMO, 2014) to obtain the critical Froude number corresponding to the threshold of surf-riding for regular waves. However it is pointed out that the Froude-Krylov component has a tendency to overestimate the amplitude of the wave-induced surge force. If a captive model experiment in a towing tank or a numerical test using CFDs is available, more accurate and reliable prediction can be achieved. However they are time- and cost- consuming methods for the ship design in an early stage, so a simple formula for the correction of the Froude-Krylov force is useful. In this reason, one proposal was submitted to IMO, as an alternative to model experiments and CFD simulations in the second-generation intact stability criteria, to introduce an empirical correction coefficient, $\mu_x$, for the linear Froude-Krylov calculation (see Eq.3). This coefficient is aimed to consider the diffraction effect missing in the Froude-Krylov assumption, and is expressed as functions of $C_m$ and $C_b$ as shown in Eq.(4) (Ito et al., 2014) (IMO, 2014).

$$f = \rho g k \frac{H}{2} \sqrt{F_C^2 + F_S^2} \tag{1}$$

$$F_c = \int_{AE}^{FE} S(x) e^{-kd(x)/2} \sin kx dx \tag{2}$$

$$F_S = \int_{AE}^{FE} S(x) e^{-kd(x)/2} \cos kx dx$$

$\rho$: density
$g$: gravity
$k$: wave number
$H$: wave height
$AE$: ship aft end
$FE$: ship fore end
$S(x)$: sectional under-water area
$d(x)$: sectional draught

$$f = \rho g k \frac{H}{2} \mu_x \sqrt{F_C^2 + F_S^2} \tag{3}$$

Here $\mu_x$ is an empirical correction coefficient derived from several captive model tests using different types of ship.

$$\begin{aligned} \mu_x &= 1.46 C_b - 0.05 && C_m < 0.86 \\ &= (5.76 - 5.00 C_m) C_b - 0.05 && 0.86 < C_m < 0.94 \\ &= 1.06 C_b - 0.05 && C_m \geq 0.94 \end{aligned} \tag{4}$$

$C_b$: block coefficient
$C_m$: midship section cefficient

## 3. SUBJECT SHIP

It is important to investigate the accuracy of CFD solvers when trying to discuss a hull form effect on the wave surging force with CFD results. The ONR tumblehome, which is a wave-piercing high-speed mono hull vessel and is prone to suffer surf-riding/broaching because of her small resistance, is selected as the subject ship because a comprehensive experimental data regarding the broaching phenomenon is available. (e.g. Umeda et al. (2008), Hashimoto et al. (2011)) The original hull of the ONR tumblehome is so slender that the midship coefficient, $C_m$, and the block coefficient, $C_b$, are small as compared to conventional commercial ships. Principal

particulars of the subject ship are shown in Table 1.

In this study, a naked hull that was not equipped with bilge keels, shaft brackets and rudders is used. The subject ship is designed for a twin screw propulsion system, so relatively large centre skeg is installed. In order to investigate the effect of ship fineness coefficients ($C_m$ and $C_b$) used in the correction coefficient, a series of hulls are artificially generated by changing the under-water hull form systematically as shown in Fig.1 and Table 2. In the hull form generation, the original length, breadth and depth of the ship are kept. Since the sonar-dome and transom stern shapes are not simple/smooth, these parts are not modified from the original design.

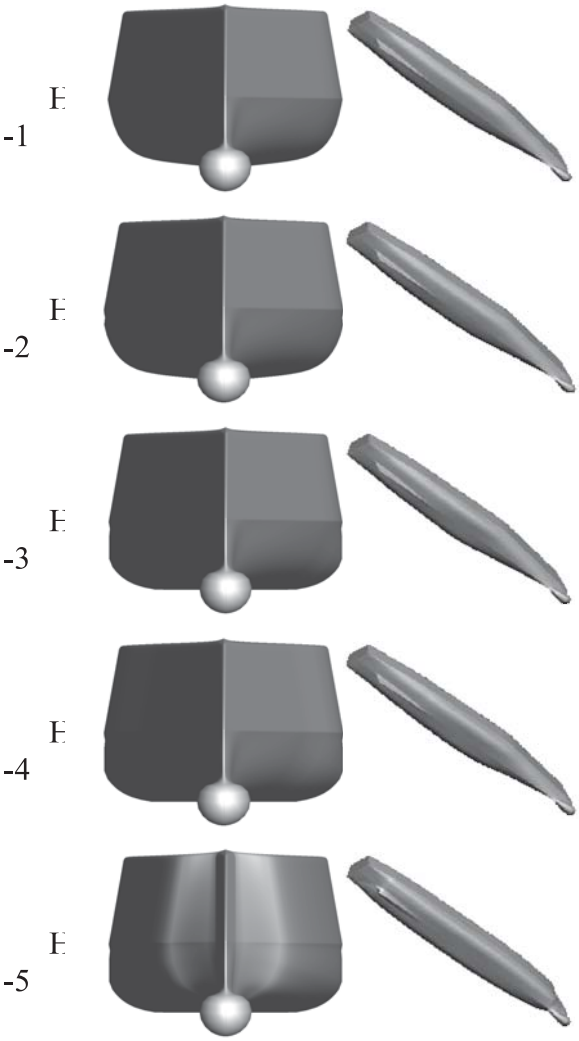


Figure 1 Geometry of the hulls

Table 1 Principal Particulars

| | |
|---|---|
| Length: $L$ | 154.0 m |
| Breadth: $B$ | 18.8 m |
| Depth: $D$ | 14.5 m |
| Draught: $d$ | 5.5 m |
| Volume: $V$ | 8562 $m^3$ |
| Block coefficient: $C_b$ | 0.535 |
| Midship section cefficient: $C_m$ | 0.835 |
| Radius of gyration in pitch: $\kappa_{yy}/L$ | 0.25 |

Table 2 Parameters of the hulls

| name | $C_m$ | $C_b$ |
|---|---|---|
| H-1 (original hull) | 0.835 | 0.539 |
| H-2 | 0.880 | 0.546 |
| H-3 | 0.950 | 0.556 |
| H-4 | 0.950 | 0.571 |
| H-5 | 0.950 | 0.695 |

## 4. CFD METHOD

### 4.1 RaNS solver

CFDShip Iowa ver.4.5 (Carrica et al., 2006) (Tahara et al., 2006) is used for numerical computation. CFDShip Iowa solves the RaNS equations using a blended k-ω/k-ε model for turbulence. The free surface is captured using a single-phase level set approach, in which the air/water interface is the zero level set distance function. The domain is discretized using multi-block structured grids. The capability of the overset is fully dynamic, which enables to simulate large amplitude motions in waves. Numerical methods include a finite difference discretization, with second-order upwind discretization for the convection term and second-order centered scheme for the viscous terms. The temporal terms are discretized using the second-order backwards Euler scheme. Incompressibility is imposed by the strong pressure/velocity coupling by using PISO. Regular waves are implemented through initial and boundary conditions. The fluid flow equations are solved in an earth-fixed inertial reference system, while the rigid body equations are done in the body-fixed system, so

forces and moments are projected to perform the integration of the rigid body equations of motion, which are solved iteratively. The SUGGAR module (Noack, 2007) is used for overset connectivity treatment and the PETSc (http://www.mcs.anl.gov/petsc/) is done to solve large simultaneous equations efficiently.

### 4.2 Grid

The overset grid design consists of 3 grids as shown in Fig.2. Two double-O boundary layer grids model the starboard and port sides of the hull to solve the asymmetric problem due to heeling. Cartesian grid is used as the background for the free surface and the wave propagation. Since the ship motion of heave and pitch is not small in steep waves even the encounter frequency is low, overset grids to accurately capture their effects might be needed to improve the prediction accuracy of the wave-induced surge force. The number of grid points is shown in Table 3. Since the total number is about 1 million, current laptop computers are sufficient enough to obtain CFD solutions. A mobile workstation of Dell Precision M6800 (Intel i7-4800MQ @2.7GHz) is used for this study.

### 4.3 Numerical condition

Numerical simulation using the overset grid RaNS solver is performed to obtain the wave-induced surge force acting on the subject ship running in pure following waves. Heave and pitch motions are solved in the CFD simulation, but other 4 degrees of surge, sway, roll, and yaw are fixed. Numerical conditions are shown in Table 4. Firstly the wave-induced surge force without heel is demonstrated to discuss the influence of hull form parameters, and then the influence of heel angle, $\phi$, is also demonstrated. The wave length to ship length ratio, $\lambda/L$, of 1.25 is used in all the simulations because surf-riding and broaching phenomena are frequently observed in a free-running model experiment with this wave length to ship length ratio (Umeda et al., 2008), and the experimentally confirmed critical Froude number for the surf-riding was about 0.35 for $\lambda$/L of 1.25 and wave steepness, $H/\lambda$, of 0.05.

Table 3 Number of grid points

| Domain | x*y*z direction | Grid points |
|---|---|---|
| Ship(S) | 72*44*54 | 171,072 |
| Ship(P) | 72*44*54 | 171,072 |
| Background | 95*67*116 | 738,340 |
| Total | | 1,080,484 |

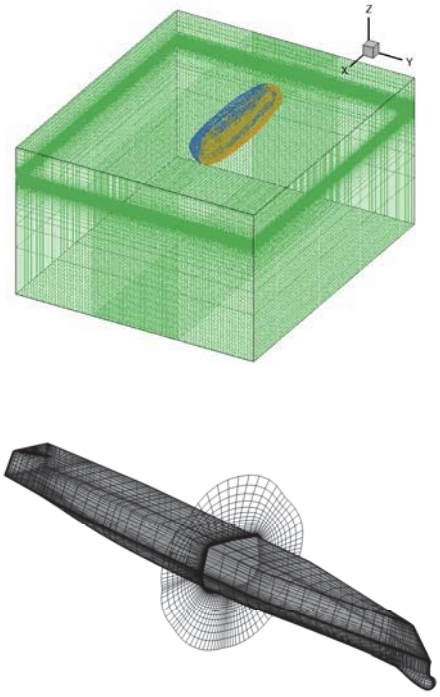

Figure 2 Computational grids

Table 4 Numerical condition

| $F_n$ | $\phi$ [deg] | $\lambda/L$ | $H/\lambda$ |
|---|---|---|---|
| 0.35 | 0 | 1.25 | 1/40 |
| 0.35 | 0 | 1.25 | 1/20 |
| 0.35 | 10 | 1.25 | 1/40 |
| 0.35 | 10 | 1.25 | 1/20 |
| 0.35 | 20 | 1.25 | 1/40 |
| 0.35 | 20 | 1.25 | 1/20 |
| 0.35 | 30 | 1.25 | 1/40 |
| 0.35 | 30 | 1.25 | 1/20 |

## 5. RESULTS AND DISCUSSION

Prior to the investigation of the influence of hull form on the wave-induced surge force, the accuracy of the overset grid CFD solver is validated for the original hull (H-1) by comparing with an existing captive model experiment by Hashimoto et al. (2011). In this experiment, a two-meter ship model is used and all the appendages are removed as done in the CFD computation. Comparisons of time histories of wave-induced surge force, heave, and pitch for the wave steepness of 1/40 and 1/20 are shown in Figs.3-4. The non-dimensional time, $t'=t/T$, of 0 means the moment when the centre of ship gravity passes a wave trough. Here the wave-induced surge force is obtained by subtracting the resistance in calm water at the same Froude number from the measured/calculated surge force in following waves. The wave-induced heave and pitch motions are obtained by the same procedure.

The CFD results show fairly good agreement in the wave-induced surge force and in vertical motions for both wave steepness. Therefore it could be concluded that it is possible to use the same RaNS solver, overset grid treatment, numerical models, and computational grids, to investigate the influence of hull form parameters on the wave-induced surge force in regular following seas.

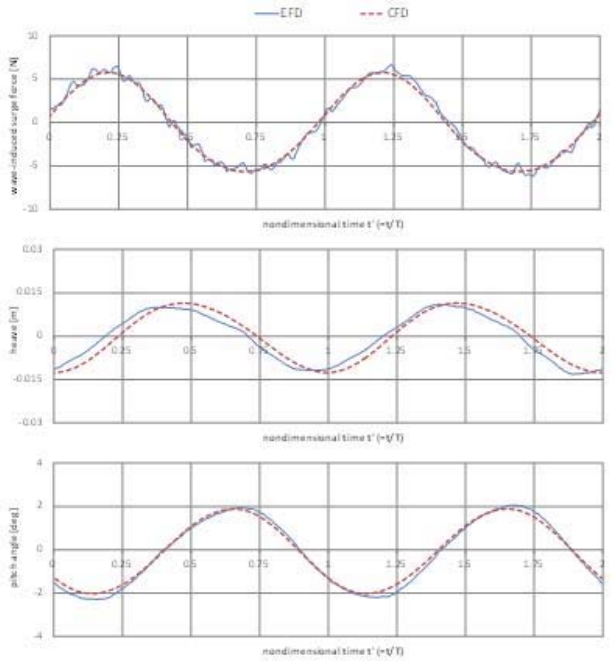


Figure 3 Comparison of wave-induced surge force, heave and pitch motions for the original hull form with $H/\lambda$=1/40

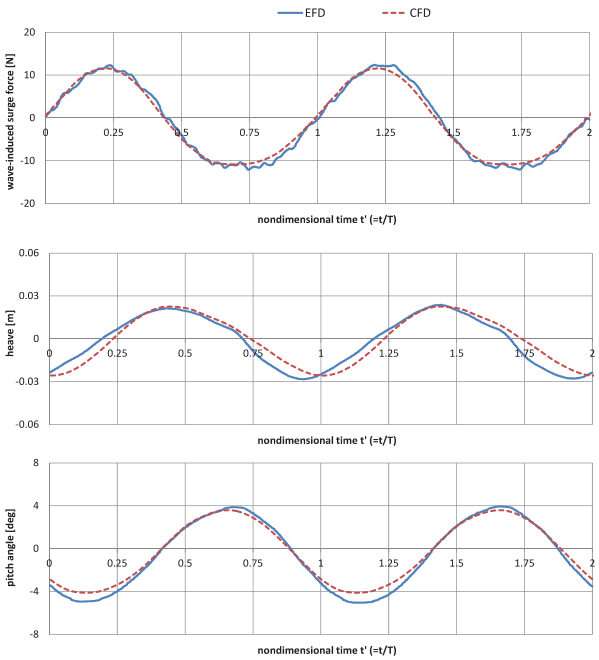


Figure 4 Comparison of wave-induced surge force, heave and pitch motions for the original hull form with $H/\lambda$=1/20

### 5.1 Influence of $C_m$ and $C_b$

The CFD simulations are performed for the hull forms derived from the original one, i.e. H-2 to H-5 those have different $C_m$ and $C_b$ values. Because the underwater hull form is modified, the ship volume for the same draught is changed, but we impose the original draught for all hulls in the CFD simulation. Comparisons of CFD results of the wave-induced surge force are shown in Figs.5-6. Here the resistance in calm water of the original hull form in calm water is subtracted from all the calculated data. Therefore the vertical shift of the mean of the wave exciting force is regarded as the increase of the resistance in calm water due to the hull form modification, so the maximum shift can be found in the most-blunt hull (H-5). The amplitude of the wave surging force has a tendency to slightly increase with the fatness of the hull, but it is negligibly small. It is noted that the linearity of the wave-induced surge

force is not confirmed for the H-5 hull. Major difference between wave steepness of 1/40 and 1/20 can be found near wave up-slope position.

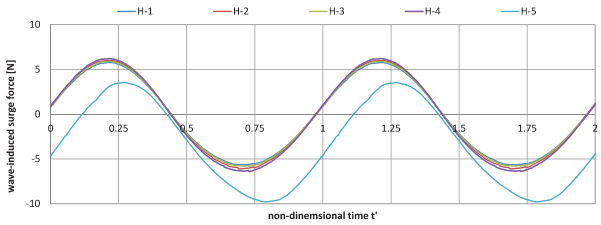


Figure 5 Comparison of wave-induced surge force for five different hull forms with $H/\lambda$=1/40

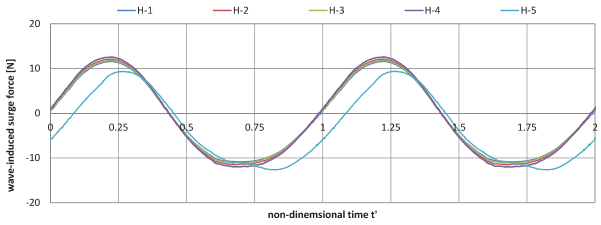


Figure 6 Comparison of wave-induced surge force for five different hull forms with $H/\lambda$=1/20

The CFD result of wave height and pressure on the underwater hull is shown in Fig.7. The ship is located in the wave down-slope potion where the wave presses the ship most strongly. It is difficult to find differences in the wave height distributions among H-1 to H-4. This means that the hull form modification, for H-1 to H-4, has few influences on the wave diffraction, ship-generated waves and their interference. In the result for the H-5 hull bloated over a considerable range, the wave diffraction and bow- and stern- generated waves are much prominent compared to H-1 to H-4 cases. Therefore the wave height distribution is different from the original sinusoidal wave. This might be a possible reason of significant change of the wave-induced surge force for the H-5 hull. The pressure distribution on the underwater hull looks not so different for H-1 to H-3. However, in the H-4 result, high-pressure region appears differently from those of H-1 to H-3, and the appearance of the pressure distribution becomes much different from others in the H-5 result. Regarding the H-5 hull, the different pattern of the pressure at bow and stern areas could be the reason to explain the phase difference of the wave-induced surge force found in Fig.6.

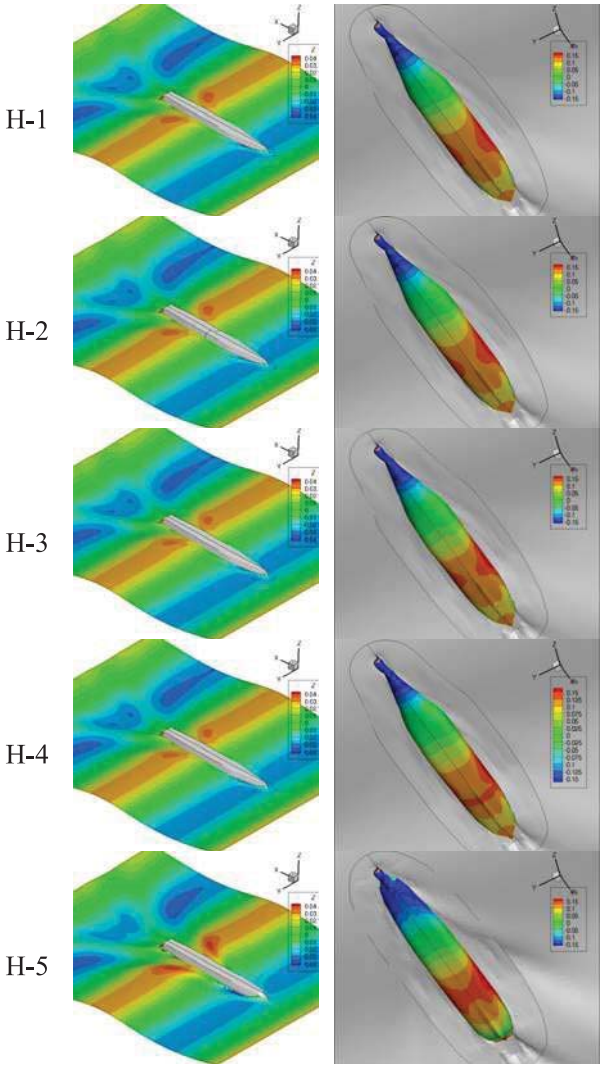


Figure 7 Contour maps of wave height and pressure with $H/\lambda$=1/20

Table 5 shows the non-dimensional amplitude of the wave-induced surge force in following seas, $X'_a = X_a / (\rho g V \times H / \lambda)$ , obtained by the CFD and the linear Froude-Krylov calculations. Here the individual volume is used for each hull. The CFD simulation, which shows good agreement with the experimental result, provides much smaller values than the Froude-Krylov force in all

conditions. This means that the linear Froude-Krylov calculation would significantly overestimate the amplitude of the wave exciting force in following waves and hence the danger of surf-riding could be overestimated. Table 6 shows the correction coefficient for the linear Froude-Krylov calculation, which is calculated by the existing correction formula of Eq.4. It would be reasonable to assume the present CFD result is accurate enough, if so the correction coefficient $\mu_x$ should coincide with the value of CFD/FK. From the results of H-1 to H-3, in which $C_m$ value is mainly changed, CFD/FK value does not always decrease with the increase of $C_m$ while $\mu_x$ decreases monotonically. From the results of H-3 to H-5, with the same $C_m$ but different $C_b$, the CFD/FK value decreases with the increase of $C_b$ while $\mu_x$ increases oppositely.

Table 5 Estimated amplitude of the wave-induced surge force

| hull | H/λ | X'a (CFD) | X'a (FK) | EFD/CFD | EFD/FK |
|---|---|---|---|---|---|
| H-1 | 0.025 | 1.246 | 1.546 | 1.024 | 0.826 |
| H-2 | 0.025 | 1.231 | 1.557 | | |
| H-3 | 0.025 | 1.299 | 1.574 | | |
| H-4 | 0.025 | 1.291 | 1.585 | | |
| H-5 | 0.025 | 1.093 | 1.412 | | |
| H-1 | 0.05 | 1.234 | 1.546 | 1.055 | 0.842 |
| H-2 | 0.05 | 1.211 | 1.557 | | |
| H-3 | 0.05 | 1.268 | 1.574 | | |
| H-4 | 0.05 | 1.258 | 1.585 | | |
| H-5 | 0.05 | 0.903 | 1.412 | | |

Table 6 Evaluation of the correction coefficient

| hull | H/λ | $C_m$ | $C_b$ | CFD/FK | $\mu_x$ |
|---|---|---|---|---|---|
| H-1 | 0.025 | 0.837 | 0.539 | 0.806 | 0.737 |
| H-2 | 0.025 | 0.88 | 0.546 | 0.790 | 0.693 |
| H-3 | 0.025 | 0.95 | 0.556 | 0.825 | 0.539 |
| H-4 | 0.025 | 0.95 | 0.571 | 0.815 | 0.555 |
| H-5 | 0.025 | 0.95 | 0.695 | 0.774 | 0.687 |
| H-1 | 0.05 | 0.837 | 0.539 | 0.798 | 0.737 |
| H-2 | 0.05 | 0.88 | 0.546 | 0.777 | 0.693 |
| H-3 | 0.05 | 0.95 | 0.556 | 0.806 | 0.539 |
| H-4 | 0.05 | 0.95 | 0.571 | 0.794 | 0.555 |
| H-5 | 0.05 | 0.95 | 0.695 | 0.639 | 0.687 |

These results indicate that the existing correction formula, using $C_m$ and $C_b$ as variables, cannot reasonably explain the influence of the hull form on the wave-induced surge force. Although the current correction formula is based on several captive model tests, the correction coefficient would be only acceptable for the original hull (H-1) and the bluntest hull (H-5). This might be because there is a certain correlation between $C_m$ and $C_b$ values for well-designed ships while such correlation is neglected in the ship hull generation in the present study. However the comparison results show that the current correction formula would be only applicable for limited hull design and does not fully explain the influence of hull form on the wave-induced surge force. Therefore further efforts, to improve/reconstruct the formula using other hull form parameters or additional elements, are expected to realize more rational correction for the regulatory use in the second-generation intact stability criteria.

## 5.2 Influence of L/B

In order to find more appropriate hull form parameters and/or other elements missing in the current correction formula, the influence of $L/B$ ratio is investigated because the diffraction force would be an important element to improve the prediction accuracy. For this purpose three fattening hulls are additionally generated by stretching the original hull in y-direction uniformly, and the stretched breadths are 1.1, 1.2 and 1.3 times of the original breadth as shown in Table 7 and Fig.8. The projected area to the y-z plane and the entrance angle of the bow becomes larger, so the diffraction effect becomes more significant. The CFD and Froude-Klyrov calculations as well as the correction coefficient are shown in Table 8. The correction coefficient is constant because the $C_m$ and $C_b$ values are the same, and the ratio of CFD and the Froudel-Krylov force shows the same tendency. Therefore it is confirmed that the diffraction effect is not a dominant, so $L/B$ or bow entrance angle is not a candidate for the improvement of the correction formula. Further investigation is

desired to develop a reasonable correction formula to be applicable for any hull forms.

Table 7 Parameters of the hulls

| Hull | *B* | *L/B* | Entrance angle [deg] |
|---|---|---|---|
| H-1 (original hull) | 18.8 | 8.19 | 19.0 |
| H-6 | 20.7 | 7.45 | 20.8 |
| H-7 | 22.6 | 6.83 | 22.7 |
| H-8 | 24.4 | 6.30 | 24.5 |

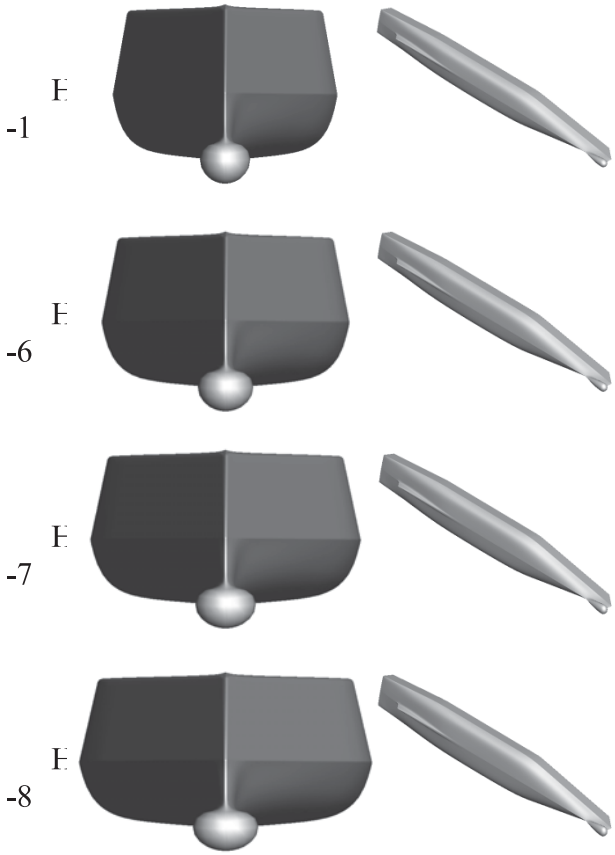


Figure 8 Geometry of the hulls

Table 8 Influence of *L/B*

| hull No. | H/λ | X'a (CFD) | X'a (FK) | CFD/FK | $\mu_x$ |
|---|---|---|---|---|---|
| H-1 | 0.025 | 1.246 | 1.546 | 0.806 | 0.737 |
| H-6 | 0.025 | 1.235 | 1.545 | 0.799 | 0.737 |
| H-7 | 0.025 | 1.234 | 1.544 | 0.799 | 0.737 |
| H-8 | 0.025 | 1.231 | 1.542 | 0.798 | 0.737 |
| H-1 | 0.050 | 1.234 | 1.546 | 0.798 | 0.737 |
| H-6 | 0.050 | 1.214 | 1.545 | 0.786 | 0.737 |
| H-7 | 0.050 | 1.203 | 1.544 | 0.779 | 0.737 |
| H-8 | 0.050 | 1.202 | 1.542 | 0.780 | 0.737 |

### 5.3 Influence of ship motion

In order to find out the major element to improve the prediction accuracy of wave-induced surge force, the influence of ship motion is examined. The CFD simulation is executed without solving the heave and pitch motions. Time histories of the calculated wave-induced surge force for the original hull is shown in Figs.9-10. Here the steady sinkage and trim in calm water at the same Froude number is neglected, but it is confirmed that their effect is negligibly small at least in the tested condition. These graphs clearly show the neglect of the ship vertical motion significantly affects both the amplitude and the phase of the wave-induced surge force. Therefore the heave and pitch motions should be included for the accurate prediction. However majority of the ship motion here is a component due to hydrostatic balancing in heave and pitch because the encounter frequency is very low and the ship length is comparable to the ship length. Therefore CFD simulation should be performed for the prescribed ship attitude obtained as hydrostatically balanced position in waves, to extract the dynamic effect of ship motion which is neglected in the Froude-Kryloy calculation

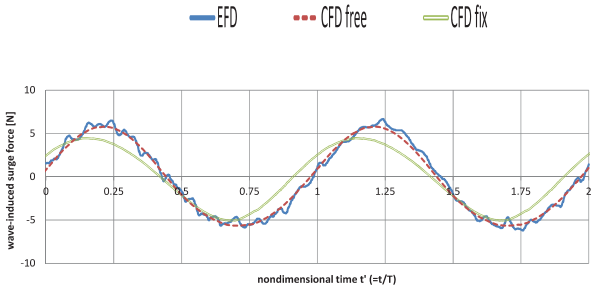


Figure 9 Influence of heave and pitch motions with $H/\lambda$=1/40

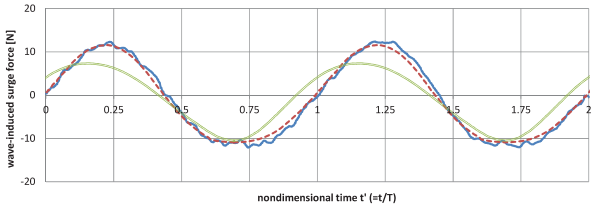


Figure 10 Influence of heave and pitch motions with $H/\lambda$= 1/20

### 5.4 Influence of heel angle

All the discussions until here are done for the ship in upright condition. Once broaching happens, violent yaw motion is induced so that a ship could largely heel due to the centrifugal force. For direct stability assessment of broaching, numerical prediction of the wave-induced surge force in largely heeled condition is also important to quantitatively assess the danger of broaching. Therefore the CFD simulation is executed for the original hull with 10, 20, and 30 degrees of heel angle. The estimated amplitudes of the wave-induced surge force are compared with an existing model experiment by Hashimoto et al. (2011) and their results are shown in Table 9. The experimental result of the amplitude of the wave-induced surge force does not change so much with the increase of heel angle up to 30 degrees. The CFD result can capture this trend and the maximum error is 8.2% and the mean error is 5.2%. The error does not increase with the heel angle, so the overset grid RaNS solver used in this study has possibility to be applicable for the direct stability assessment of surf-riding/broaching phenomenon as the third level of the direct stability assessment.

Table 9 Influence of heel angle

| hull No. | H/λ | ϕ | X'a (CFD) | X'a (EFD) | EFD/CFD |
|---|---|---|---|---|---|
| H-1 | 0.025 | 0 | 1.246 | 1.277 | 1.024 |
| H-1 | 0.05 | 0 | 1.234 | 1.302 | 1.055 |
| H-1 | 0.025 | 10 | 1.248 | 1.328 | 1.064 |
| H-1 | 0.05 | 10 | 1.228 | 1.329 | 1.082 |
| H-1 | 0.025 | 20 | 1.187 | 1.262 | 1.062 |
| H-1 | 0.05 | 20 | 1.222 | 1.261 | 1.032 |
| H-1 | 0.025 | 30 | 1.181 | 1.237 | 1.047 |
| H-1 | 0.05 | 30 | 1.228 | 1.197 | 0.975 |

## 6. CONCLUSIONS

The influence of hull parameters on the wave-induced surge force in following seas is investigated using an overset grid RaNS solver. The importance of $C_m$ and $C_b$ is investigated with a series of derived hull forms from the ONR-tumblehome vessel. It is recognized that increasing of $C_b$ affects the amplitude of wave-induced surge force while $C_m$ does not so. Since it is reconfirmed that the linear Froude-Krylov force significantly overestimates the amplitude of wave-induced surge force, reasonable correction formulae are highly desired to be used in the level two vulnerability criteria for broaching. Therefore current proposal of a correction formula is evaluated by CFD-based numerical tests. As a result, it is demonstrated that the current correction formula has limitation and cannot reasonably explain the influence of the hull form on the wave-induced surge force. Further investigation on the influence of $L/B$, heave and pitch motions, and heel angle is also performed. The $L/B$ ratio and the heel angle are not influential but the consideration of ship motion is an important element for the accurate prediction of the wave-induced surge force at least for the subject ship. Further comprehensive research is necessary to develop and propose more valid and reliable correction formula to be applicable to any types of ship for the second-generation intact stability criteria for broaching.

## 7. ACKNOWLEDMENTS

This work was supported by JSPS KAKENHI Grant Number 25249128 and 24360355, and was also carried out as a research activity of Goal-Based Stability Criterion Project of Japan Ship Technology Research Association in the fiscal year of 2014, funded by the Nippon Foundation. The authors thank Prof. Naoya Umeda from Osaka University for his useful discussion.

## 8. REFERENCES

Carrica, P. M., Wilson, R.V., Noack, R., Xing, T., Kandasamy, M., Shao, J., Sakamoto, N., and Stern, F. 2006, "A Dynamic Overset, Single-Phase Level Set Approach for Viscous Ship Flows and Large Amplitude Motions and Maneuvering", Proceedings of 26th Symposium on Naval Hydrodynamics,

Rome.

Hashimoto, H., Umeda, N., Matsuda, A. 2011, "Broaching prediction of a wave-piercing tumblehome vessel with twin screws and twin rudders", Journal of Marine Science and Technology, 16, pp.448-461.

IMO, "Proposed Amendments to Part B of the 2008 IS Code to Assess the Vulnerability of Ships to the Broaching Stability Failure Mode", SDC1 INF.8 ANNEX15.

IMO, "Proposal of working version of explanatory notes on the vulnerability of ships to the broaching stability failure mode", SDC1/5/4.

Ito, Y., Umeda, N. and Kubo, H., 2014, "Hydrodynamic Aspects on Vulnerability Criteria for Surf-Riding of Ships", Jurnal Teknologi, Vol. 66, No. 2, pp. 127-132.

Noack, R., 2007, "Enabling Large Amplitude and Relative Motions Through Overlapping Grids", Proceedings of 9th International Conference on Numerical Ship Hydrodynamics, Michigan.

Tahara, Y., Wilson, R.V., Carrica, P.M. and Stern, F. 2006, "RANS Simulation of a Container Ship Using a Single-Phase Level Set Method with Overset Grids and Prognosis for Extension to Self-Propulsion Simulator", Journal Marine Science and Technology, 11, pp. 209-228.

Umeda, N., Yamamura, S., Matsuda, A., Maki, A., Hashimoto, H., 2008, "Model Experiments on Extreme Motions of a Wave-Piercing Tumblehome Vessel in Following and Quartering Waves", Journal of the Japan Society of Naval Architects and Ocean Engineers, 8, pp.123-129.